第33卷 第4期 焊 接 学 报 Vol. 33 No. 4
2012年4月 TRANSACTIONS OF THE CHINA WELDING INSTITUTION April 2012

Sn-Zn-Ga-Pr钎料表面锡须的自发生长

叶 焕[1,2]， 薛松柏[1]， 薛 鹏[1]， 陈 澄[1]
(1. 南京航空航天大学 材料科学与技术学院，南京 210016;
2. 马里兰大学 先进寿命周期工程研究中心，美国 马里兰 20742)

摘 要：结合扫描电镜与电子能谱分析了稀土元素对无铅钎料显微组织的影响. 结果表明，当无铅钎料中的稀土添加过量，会诱发锡须在无铅合金表面的自发生长. 在向Sn-9Zn-0.5Ga基体合金中添加0.7%(质量分数)的稀土元素镨(Pr)后，仅需室温时效12 h，合金组织中的稀土相表面即发生了锡须的自发生长. 随着时效时间的延长，锡须会继续长大，其最终长度可达100 μm. 最后对过量稀土元素添加导致锡须生长的力学原因作了初步探讨，分析认为稀土相氧化所产生的微观压应力可能为锡须的生长提供了驱动力.

关键词：无铅钎料；稀土元素；锡须；驱动力
中图分类号：TG425 **文献标识码**：A **文章编号**：0253-360X(2012)04-0042-03

叶 焕

0 序 言

环境友好型材料的研发与应用趋于成熟，发达国家限制含铅材料在电子制品的使用已成为现实. 在“无铅化”逐步推进的今天，有关无铅钎料的研究与开发成为电子行业所用连接材料研究的热点课题[1,2]. 目前研究的诸多代表性无铅钎料如Sn-Ag-(Cu)，Sn-Cu，Sn-Zn钎料等虽然都有各自的优势，但到目前为止，还没有任何一种无铅钎料能够在生产应用中完全替代Sn-Pb合金[1]. 为了进一步提高无铅钎料的综合性能，许多研究人员推荐采用稀土合金化，即通过向基体合金中加入适量稀土元素(RE)的方法来提高钎料与焊点的综合性能. 稀土元素被称为金属材料的“维他命”，其化学性质活泼、原子半径较大，在合金组织中容易吸附在晶界，起到净化晶界、细化晶粒从而改善性能的变质作用. 已有报道表明，稀土元素的添加可以极大改善钎料合金的各项性能. 如Chen等人[3]研究发现向Sn-Ag-Cu钎料中添加稀土元素La，Ce时，接头的抗蠕变性能提高了7倍. 文献[4]也报道稀土元素Er，Pr等可以显著改善Sn-Ag-Cu或Sn-Cu钎料的性能. Wu等人[5]的研究也表明，稀土元素可以提高Sn-Zn钎料的抗氧化能力，有效改善其润湿性能与力学性能. 稀土元素对无铅钎料的优良改性效果的相关报道有很多. 然而最近有部分研究发现，稀土元素可能会导致无铅钎料中的锡须生长. 如Jiang等人[6]发现Sn-Cu钎料中稀土元素Nd的引入会导致合金镀层表面锡须的大量生长. Chuang[7]也发现向Sn-Ag-Cu合金中添加铈时导致钎料中锡须的快速生长. 并且他们通过进一步研究认为向无铅钎料中加入Zn元素可以有效抑制锡须的生长. 锡须是一种良好的导电体，它的生长会导致通电器件的短路与电弧放电，严重威胁着电子设备的长期可靠性.

锡须生长一般发生在镀层表面，在钎料上的直接生长还是一个全新的课题. 文中通过试验研究在含锌和稀土的Sn-Zn-Ga-Pr钎料中发现了锡须自发生长现象，这一新的发现对前人提出的抑制锡须生长的方法提出了挑战，为有关锡须生长问题的研究提供了新的思路.

1 试验方法

由于稀土元素Pr在高温下容易氧化烧损，因此研究中首先制备出Sn-5% Pr(质量分数)二元低熔点中间合金，然后把Sn-5% Pr中间合金、纯锡、纯锌与纯镓按计算好的比例均匀混合，放入氧化铝陶瓷坩埚中并置于井式炉加热熔化，熔炼过程中不断搅

收稿日期：2011-04-07
基金项目：江苏省普通高校研究生科研创新计划资助项目(CXZZ11-0208)；南京航空航天大学博士学位论文创新与创优基金资助项目(BCXJ11-08)；2010年江苏省企业研究生工作站资助项目

拌并采用 KCl + LiCl 熔盐覆盖进行保护,再保温、浇注并冷却,制备试验所需 Sn-9Zn-0.5Ga-0.7Pr 钎料块. 然后在 SAT-5100 可焊性测试仪自带的坩埚中将制得的钎料块进行二次重熔,用该设备配备的热电偶精确控制最高加热温度在 235 ℃模拟钎料合金的回流工艺. 将得到的钎料试样进行预磨、抛光与腐蚀,最后在环境湿度下室温时效不同时长(0,12 h,30,60,90 d) . 采用扫描电镜(SEM) 与电子能谱(EDS) 对所得试样进行组织观察与成分分析.

2　试验结果及分析

图 1a 为 Sn-9Zn-0.5Ga-0.7Pr 钎料合金的回流组织形貌. 由图 1a 可知,合金组织表现出典型的 Sn-Zn 共晶体系的形貌特征,即灰色的 β-Sn 基体与黑色的针状富锌相交叠在一起所形成的共晶组织. 除此之外,基体组织中还出现了花瓣状的新相. EDS 分析显示该析出相为锡和镨所形成的金属间化合物,Sn,Pr 原子比为 3∶1,如图 1b 和表 1 所示. 结合 Sn-Pr 相图[8] 分析,可以确定该新相为 $PrSn_3$ 稀土相.

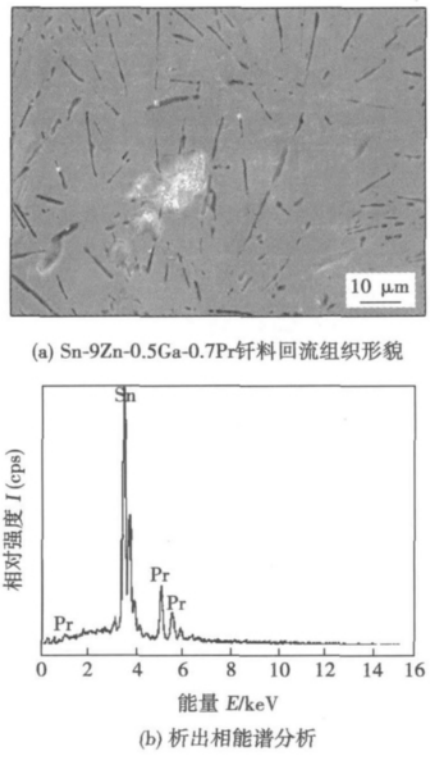

图 1　Sn-9Zn-0.5Ga-0.7Pr 钎料回流组织形貌与能谱分析

Fig. 1　SEM image of Sn-9Zn-0.5Ga-0.7Pr solders and related EDS analysis

将回流试样在环境氛围下室温时效 12 h,得到的扫描形貌如图 2a 所示. 发现在稀土相表面长出了一些长短不一的亮银色针状金属须,能谱分析(图 2b) 显示该须状物为纯锡,即锡须. 由图 2a 可知锡须的长度都很小,最长的大约为 3 μm,直径也都非常小,难以精确测量. 另外在稀土相表面还出现了许多米粒状的细小颗粒,初步判断认为该颗粒为锡须的萌芽状态,在后续生长中继续长大为锡须.

表 1　元素能谱分析结果(%)

Table 1　Elements result by EDS analysis

元素	质量分数	原子分数
Sn	72.51	75.80
Pr	27.49	24.20
总量	100.00	100.00

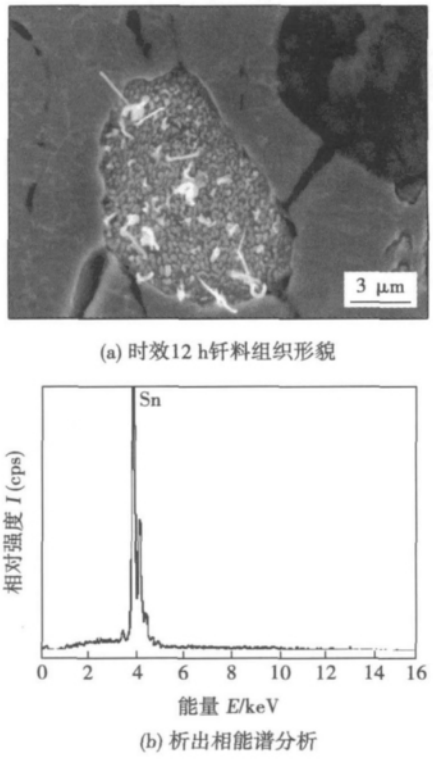

图 2　室温时效 12 h 后钎料扫描形貌与能谱分析

Fig. 2　SEM image of solder exposed for 12 hours and related EDS analysis

图 3 所示为试样在时效 60 d 后得到的组织与锡须形貌. 对比图 3 与图 2a 可发现,在稀土相表面长出了更多的锡须,锡须的形态也发生了变化,除了之前出现的直线形生长,还出现了明显的不规则型长大,如弯折生长、缠绕生长等. 并且锡须的长度与粗度也都有明显长大. 对试样中的锡须在多个视场下的最长长度取平均值可发现,室温下保存 60 d,锡须长度可长到近 70 μm. 电子行业中多个标准认为

50 μm 是锡须生长的临界值，当长度超过 50 μm 时即可认为造成器件失效[9]. 因此文中发现的这一新问题可能对电子器件的长期可靠性造成较大的危害，需要进行深入的研究.

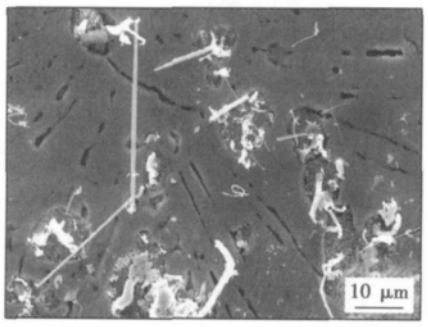

图 3 室温时效 60 d 后钎料组织形貌

Fig. 3 SEM image of solder exposed for 60 hours

对试样继续进行时效处理，保温 90 d 后观察试样表面形貌，发现锡须的平均长度与时效 60 d 时相比，仅有略微上升，表明锡须的生长逐渐停止. 但是仍有少量锡须可生长至长达 100 μm，给电子产品带来了极大的失效风险.

有关镀层上锡须产生的原因，目前还没有一个完善的机制可以被科学界所普遍接受[10]. 对于 Sn-Zn-Ga-Pr 体块钎料表面的锡须生长，基于材料的性质与试验分析，研究认为其驱动力可能源自于稀土相的快速氧化. 前面提到稀土元素化学性质活泼，在空气中就很容易氧化. 钎料中所含稀土元素在室温时效时与空气中的 O_2 反应，O 原子在稀土相晶格内部的扩散会导致其体积的增大，但是这种体积膨胀又会受到周围 β-Sn 基体的限制，导致在 Sn-Pr 化合物内部产生压应力[9]. 随着氧化的深入，压应力会逐渐增大. 当内部压应力达到一个临界值，它会在 Sn-Pr 化合物表面氧化层的某些薄弱的地方释放压应力，驱动 Sn 原子从这些薄弱的点不断被挤出，从而形成锡须. 由于氧化可以持续相当长一段时间，可以为锡须的生长提供持续驱动力，因此锡须可以在较长时间内持续生长，直到内应力完全耗尽.

3 结 论

(1) 稀土元素 Pr 在 Sn-Zn-Ga-Pr 钎料组织中以稀土相 Sn-Pr 金属间化合物的形式存在.

(2) 室温时效过程中锡须可以在较短时间内在钎料表面萌生. 随着时效时间的延长，锡须表现出持续生长，锡须的数量、长度与横截面积都有增大趋势，并且锡须的生长形态也趋于不规则化.

(3) 锡须的生长与稀土相的氧化有关，稀土元素 Pr 与空气中 O_2 的反应会导致稀土相体积的增大，体积膨胀会受到周围 β-Sn 基体的限制，导致在 Sn-Pr 化合物内部产生压应力，为锡须的生长提供驱动力.

参考文献:

[1] Suganuma K. Advances in lead-free electronics soldering [J]. Current Opinion in Solid State and Materials Science, 2001, 5(1): 55 - 64.

[2] Ye Huan, Xue Songbai, Zhang Liang, *et al*. Reliability evaluation of CSP soldered joints based on FEM and taguchi method [J]. Computational Materials Science, 2010, 48(3): 509 - 512.

[3] Chen Zhigang, Shi Yaowu, Xia Zhidong, *et al*. Study on the microstructure of a novel lead-free solder alloy SnAgCu-RE and its soldered joints [J]. Journal of Electronic Materials, 2002, 31(10): 1122 - 1128.

[4] Hao Hu, Shi Yaowu, Xia Zhidong, *et al*. Microstructure evolution SnAgCuEr lead-free solders under high temperature aging [J]. Journal of Electronic Materials, 2008, 37(1): 2 - 8.

[5] Wu C M L, Wong Y W. Rare-earth additions to lead-free electronic solders [J]. Journal of Materials Science: Materials in Electronics, 2007, 18(s): 77 - 91.

[6] Jiang Bo, Xian Aiping. Observations of ribbon-like whiskers on tin finish surface [J]. Journal of Materials Science-Materials in Electronics, 2007, 18(5): 513 - 518.

[7] Chuang Tunghan. Rapid whisker growth on the surface of Sn-3Ag-0.5Cu-1.0Ce solder joints [J]. Scripta Materialia, 2006, 55(11): 983 - 986.

[8] Baker H, Okamoto H. Alloy phase diagrams [M]. USA: American Society of Mechanical Engineers Handbook, 1992.

[9] Ye Huan, Xue Songbai, Zhang Liang, *et al*. Sn whisker growth in Sn-9Zn-0.5Ga-0.7Pr lead-free solder [J]. Journal of Alloys and Compounds, 2011, 509(5): 52 - 55

[10] 江 波，冼爱平. 锡镀层表面晶须问题的研究现状与进展 [J]. 表面技术，2006，35(4)：1 - 4.
Jiang Bo, Xian Aiping. Review of whisker growth in tin coating [J]. Surface Technology, 2006, 35(4): 1 - 4.

作者简介：叶 焕，男，1986 年出生，博士研究生. 主要从事电子封装可靠性的相关研究工作. 发表论文 5 篇. Email: yeehone@umd.edu

Study on sub-arc X-ray welding image defect segmentation algorithm and defect model GAO Weixin[1], HU Yuheng[2], MU Xiangyang[1], WANG Zhi[3] (1. Shanxi Key Laboratory of Oil-Drilling Rigs Controlling Technique, Xi'an Shiyou Univerisy, Xi'an 710065, China; 2. Department of Electrical & Computer Engineering, University of Wisconsin-Madison, Madison 53705, USA; 3. National Laboratory of Industrial Control Technology, Zhejiang University, Hangzhou 310027, China). pp 37 - 41

Abstract: Regarding the present problems that the traditional image segmentation algorithm can only achieve a low successful defect segmentation ratio for the strong noise and low contrast of submerged-arc x-ray image, an efficient X-ray radiography image analysis algorithm is developed for the task of segmentation of submerged-arc welding defects. In the new algorithm, the defect is treated as noise and a new concept-"gray density" is put forward for calculation convenience. Tested with 100 X-ray radiography images obtained from a real factory, the proposed algorithm can increase successful segmentation ratio and achieves a successful ration of 95%. Based on the clustering segmentation algorithm, a high dimension space defect mathematical model is presented. The model makes the characteristic of the complexity of the form into consideration. Real examples show that the model is effective and practical. The sensitivity curve of the presented clustering segmentation algorithm is also given.

Key words: welding gap; defect; segmentation; clustering

Spontaneous growth of Sn whiskers on surface of Sn-Zn-Ga-Pr solders YE Huan[1,2], XUE Songbai[1], XUE Peng[1], CHEN Cheng[1] (1. College of Materials Science and Technology, Nanjing University of Aeronautics and Astronautics, Nanjing 210016, China; 2. Center for Advanced Life Cycle Engineering, University of Maryland, College Park 20742, USA). pp 42 - 44

Abstract: In spite of many beneficial effects obtained from the doping of rare earth (RE) to lead-free solders, it is newly found that an exceeded addition of RE would cause a risk of Sn whisker growth in the alloys. The results indicate that with the addition of 0.7% Pr to Sn-9Zn-0.5Ga solder, many Sn whiskers spontaneously grow from the surface of Sn-Pr phases in the bulk solder exposed for 12 hours only. And the whiskers show a continuous growth with the exposure time being increased. The final longest length of the whisker can reach 100 μm, which can lead to a serious reliability problem for electronic assemblies. Finally, the mechanical reason for whisker growth is discussed.

Key words: lead-free solder; rare earth; Sn whisker; driving force

Application of computes-aided ultrasonic phased array in inspection of weld in TKY tubular node LU Minghui, CHENG Jun, SHAO Hongliang, SUN Minglei (Key Lab of Nondestructive Testing, Ministry of Education, Nanchang Hangkong University, Nanchang 330063, China). pp 45 - 48

Abstract: Analytic geometry theories and methods were applied to found the mathematical model of welds in TKY tubular node. According to the regulation of the size, welded joints were drawn after getting weld cross-section in tubular node. The ultrasonic phased array probe profile was designed on the basis of its physical size, and ultrasonic beam was also designed. The computer-aided technology can achieve the beam coverage of welded joints, which can commendably guide the design of ultrasonic phased array inspection and evaluate ultrasonic test blind areas of weld in TKY tubular node. The blindness of setting parameters can be overcome in the course of ultrasonic phased array inspection. Tests of weld in artificial Y tubular node indicated that the combination of ultrasonic phased array imaging technology and computer-aided techniques contributed to rapid detection and evaluation of weld in tubular node.

Key words: TKY tubular joint; ultrasonic phased array; computer-aided; beam coverage

Microstructure of TiAl joints brazed with TiNiB high-temperature filler metal YANG Zhenwen, ZHANG Lixia, XUE Qing, HE Peng (State Key Lab of Advanced Welding and Joining, Harbin Institute of Technology, Harbin 150001, China). pp 49 - 52

Abstract: High-temperature filler metal of TiNiB prepared by arc melting was used as an active filler metal in vacuum brazing of TiAl alloy. The effect of brazing temperature on the microstructure evolution of the joints was studied in this paper. The TiNiB filler metal was mainly comprised of TiNi and $TiNi_3$ eutectic microstructure, in which some TiB_2 blocks appeared. The melting point of the filler metal was 1 120 ℃. The dissolution of TiAl substrate has a strong effect on interfacial structure. The TiAl alloy adjacent to brazed seam was transformed to β layer with the dissolution of TiAl substrate. The microstructure of the brazed seam was comprised of Ti-Al-Ni compounds and a little β phase. TiB_2 was transformed to TiB due to the reaction with Ti.

Key words: TiAl alloy; TiNiB filler; brazing; microstructure

Investigation on wear resistance of Fe-based composite material containing titanium ZONG Lin[1,2], LIU Zhengjun[1], LI Lecheng[1] (1. School of Material Science and Engineering, Shenyang University of Technology, Shenyang 110178, China; 2. School of Mechanical Engineering, Shenyang University of Chemical Technology, Shenyang 110142, China). pp 53 - 56

Abstract: A series of Fe-Cr-Ti-C hardfacing alloys with different Cr contents were prepared by PTA in order to develop a Fe-based wear resistant composite material. The microstructure and carbides morphology were investigated by means of scanning electron microscopy (SEM) and X-ray diffraction (XRD). The results show that the matrix transforms from austenite and ferrite to ferrite and martensite, the volume fraction of M_7C_3 and TiC increase with the Cr content being increased. In addition, the effects of Cr content on wear resistance were studied. The wear resistance of cladding layer increases with increase of Cr content. When Cr content is 20.1%, the microstructure characteristic with a high volume fraction of hexagonal M_7C_3 complex carbides and a small amount globular, exploded and agglomerated TiC particles are distributed in the lath martensite matrix with higher strength and toughness, which suggests that the cladding layer has a excellent wear resistance.